SINGULAR BEAMS IN UNIAXIAL CRYSTALS[1]

A.V. VOLYAR

V.I.Vernadsky Tavrida National University
(4, Yaltinska Str., Simferopol 95007, Ukraine)

UDC 535.212

We present a method for the generation of optical vortices nested in a singular beam that propagates along a uniaxial crystal and a polarized filter. The theoretical analysis based on solving the paraxial wave equation showed that the paraxial fundamental Gaussian beam can transform into a singular beam bearing the double charged optical vortex: the left-hand circularly polarized beam converts into the right-hand polarized beam with a positive topological charge whereas the right-hand one generates the left-hand polarized beam with a negative charged vortex. Moreover, the device can transform high-order singular beams in such a way that the negative topological charge of the vortex in the right-hand polarized beam raises by two units, but the positive vortex charge in the same beam diminishes by two units. The computer simulation of the process is accompanied by the numerous experimental results.

Introduction

The problem of phase singularities or optical vortices is not something new, suddenly arisen, in optics after M. Berry has drawn attention to the surprising properties of wavefront dislocations [1] in 1974. As far back as at the end of the 19th and at the beginning of the 20th centuries, many investigators noticed a strange behavior of the energy flow near a focal plane of a microscope in the vicinity of anomalous Airy's rings. Lines of the energy flow encircled the rings forming circles and loops even in free space (see, for example, works [2—4]). Moreover, the typical behavior of phase singularities due to light diffraction and interference is elucidated by the excellent illustrations in the fundamental works [5, 6].

Nevertheless, at the end of the 20th century, the interest in phase singularities broke out with a new force. Its source was the most quoted works [7, 8] (see also [2]) by M. Soskin and others on the simple and reliable technique to generate optical vortices nested in singular beams. A computer-generated hologram being the corner stone of the technique made it possible to form singular beams bearing an arbitrary pattern of optical vortices. This work stimulated a flow of publications. Further, these were transformed into a new branch of modern optics that has come at the moment to be called (following M. Soskin) singular optics [9].

At the same time, the computer-generated hologram technique has one drawback — the energy effectiveness of thin holograms is rather low (about 10—15% at best). In addition, static holograms generally do not permit to control and to tune a vortex position in the beam.

Here I will concentrate on the problem of the vortex generation with an anisotropic medium. This problem has been partially discussed at the moment in a number of publications [10—20]. For instance, in works [10—13], the authors used biaxial and uniaxial crystals to generate and convert Bessel beams, whereas transformation and focusing processes of Gaussian beams in those crystals were regarded in works [15—18]. The generation of a singular beam in liquid crystal cells is illustrated by works [14, 19], and the work [20] presents the eigenmodes of axisymmetric inhomogeneous anisotropic media. At the same time, the authors laid special stress on experimental results, while theoretical aspects of transformations of Gaussian singular beams in anisotropic media were minor questions.

The main purpose of the given paper is to examine the theoretical base of transmitting the paraxial Gaussian beams through a uniaxial crystal along its optical axis so to emphasize the variety of new ways of the transforming and generating of optical vortices.

Beams with Eigen Polarization and Optical Vortices

Consider, at first, the propagation of a paraxial Gaussian beam through the crystal without transformation of its structure, that is, the beam with an eigen polarization.

A monochromatic wave can be described in terms of Maxwell's equations as

$$\nabla \times \mathbf{E} = -i\frac{\mu\omega}{c}\mathbf{H},$$

$$\nabla \times \mathbf{H} = i\frac{\hat{\varepsilon}\omega}{c}\mathbf{E}, \quad \nabla(\hat{\varepsilon}\mathbf{E}) = 0, \quad \nabla\mathbf{H} = 0. \qquad (1)$$

[1] This article is dedicated to Professor Marat Soskin on the occasion of his 75th birthday.

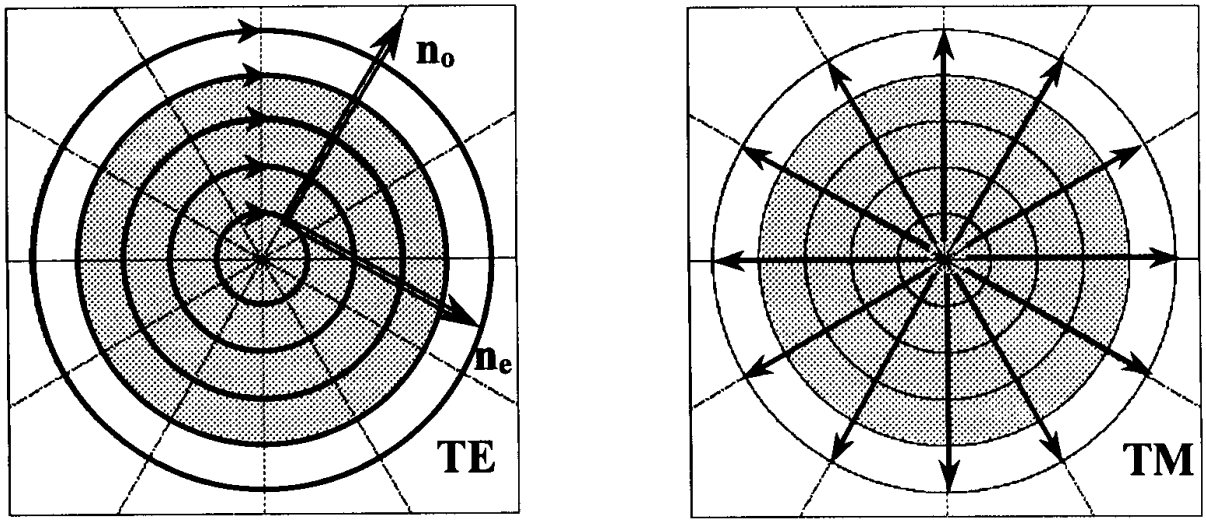

Fig. 1. Structure of the main birefringent axes n_o and n_e in the uniaxial crystal corresponding to the propagation of a light beam along the optical axis and the structure of the eigen TM and TE polarizations of the paraxial Gaussian beam

Consider the coordinate system (x, y, z) in which the permittivity tensor has the form: $\hat{\varepsilon} = \mathrm{diag}\,(\varepsilon_{jj})$ so that $\varepsilon_{11} = \varepsilon_{22} = \varepsilon$ and $\varepsilon_{33} = \varepsilon_3$. The wave equation can be written as

$$\left(\nabla^2 + k^2\hat{\varepsilon}\right)\,\mathbf{E} \;=\; -\nabla\left(\frac{\Delta\varepsilon}{\varepsilon_3}\nabla_t\mathbf{E}_t\right)\,, \qquad (2)$$

where $\nabla_t = \hat{\mathbf{x}}\,\partial_x + \hat{\mathbf{y}}\,\partial_y$, with $\hat{\mathbf{x}}$ and $\hat{\mathbf{y}}$ unit coordinate vectors of x and y axes,

$$\partial_{x,y} = \partial/\partial\,x, \partial/\partial\,y,\;\; \mathbf{E}_t = \hat{\mathbf{x}}\,E_x + \hat{\mathbf{y}}\,E_y,$$

$$k^2 = \mu\,\varepsilon\,\omega^2/c^2,\;\; \Delta\varepsilon = \varepsilon_3 - \varepsilon.$$

We are interested in the propagation of a paraxial Gaussian beam along the optical axis z. To find the paraxial equation we write

$$\mathbf{E} = \tilde{\mathbf{E}}\,(x, y, z)\,\exp\,(ikz) \qquad (3)$$

and assume: $\left|\partial_{zz}\tilde{\mathbf{E}}\right| \ll k\left|\partial_z\tilde{\mathbf{E}}\right|, k\left|\tilde{\mathbf{E}}\right|$ whence

$$\left(\nabla_t^2 + 2\,i\,k\,\partial_z\right)\,\tilde{\mathbf{E}}_t \;=\; -\,\frac{\Delta\varepsilon}{\varepsilon}\nabla_t\,\left(\nabla_t\,\tilde{\mathbf{E}}_t\right). \qquad (4)$$

As far as the longitudinal electric component $\tilde{E}_z$ is assumed small, the analysis can be restricted with transverse electric components $\tilde{\mathbf{E}}_t$.

In the ray approximation, the main axes of the crystal anisotropy lay in the plane (and perpendicularly to it) made by the given ray and the crystal optical axis [3]. It is natural to suppose that the structure of the eigen polarization of the beam has to be in keeping with that of the crystal anisotropy presented by Fig.1. Mathematically, it looks like

$$\tilde{\mathbf{E}}_{\mathrm{TE}} = r\,(\hat{\mathbf{x}}\,\sin\,\varphi\;-\;\hat{\mathbf{y}}\,\cos\,\varphi)\;G_{\mathrm{TE}}\;(r, \varphi, z)\,/Z\quad, \qquad (5)$$

$$\tilde{\mathbf{E}}_{\mathrm{TM}} = r\,(\hat{\mathbf{x}}\cos\,\varphi + \hat{\mathbf{y}}\sin\,\varphi)\;G_{\mathrm{TM}}\;(r, \varphi, z)\,/Z, \qquad (6)$$

where $G = \exp\left(i\beta_{\mathrm{TE}}\frac{r^2}{2\,Z}\right)/Z$, $G = \exp\left(i\beta_{\mathrm{TM}}\frac{r^2}{2\,Z}\right)/Z$, $Z = z - i\,z_0$, $z_0 = \frac{k\,\rho^2}{2}$, $\beta_{\mathrm{TE}} = k_0\sqrt{\varepsilon}$, $\beta_{\mathrm{TM}} = \beta_{\mathrm{TE}}\left(1 + \frac{\Delta\varepsilon}{\sqrt{\varepsilon}}\right)$, ρ is the beam waist radius.

The first field (5) is a solution of the equation:

$$\left(\nabla_t^2 + 2\,i\,k\,\partial_z\right)\,\tilde{\mathbf{E}}_{\mathrm{TE}} \;=\; 0 \qquad (7)$$

because the z-component of the transverse electric mode $\tilde{\mathbf{E}}_{\mathrm{TE}}$ is zero ($E_z = 0$ and, consequently, $\nabla_t\,\tilde{\mathbf{E}}_t = 0$ on the right side of Eq. (4)).

As can be shown by the direct substitution, expression (6) is the solution of the paraxial wave equation (4).

Using the rule $\tilde{\Psi}_{1,2} = \tilde{\mathbf{E}}_{\mathrm{TM}} \pm i\,\tilde{\mathbf{E}}_{\mathrm{TE}}$ [21], we can form the singular beam bearing optical

vortices:

$$\tilde{\Psi}_1 = \frac{r}{Z}\left\{\hat{\mathbf{c}}^+ i \sin\left(\Delta\beta\frac{r^2}{4\,Z}\right) \exp\left(-i\,\varphi\right) + \hat{\mathbf{c}}^- \times \right.$$

$$\left. \times \cos\left(\Delta\beta\frac{r^2}{4\,Z}\right) \exp\left(i\,\varphi\right)\right\} \exp\left(i\,\tilde{\beta}\frac{r^2}{2\,Z}\right), \qquad (8)$$

$$\tilde{\Psi}_2 = \frac{r}{Z}\left\{\hat{\mathbf{c}}^+ \cos\left(\Delta\beta\frac{r^2}{4\,Z}\right) \exp\left(-i\,\varphi\right) + \hat{\mathbf{c}}^- i \times \right.$$

$$\left. \times \sin\left(\Delta\beta\frac{r^2}{4\,Z}\right) \exp\left(i\,\varphi\right)\right\} \exp\left(i\,\tilde{\beta}\frac{r^2}{2\,Z}\right), \qquad (9)$$

where $\hat{\mathbf{c}}^+ = \hat{\mathbf{x}} + i\,\hat{\mathbf{y}}$, $\hat{\mathbf{c}}^- = \hat{\mathbf{x}} - i\,\hat{\mathbf{y}}$ are the orts of the circularly polarized basis, $\tilde{\beta} = \beta_{\mathrm{TE}} + \frac{\Delta\beta}{2}$, $\Delta\beta = k_0\frac{\Delta\varepsilon}{\sqrt{\varepsilon}}$.

We can see from Eqs. (8) and (9) that the singular beam contains two local optical vortices with opposite topological charges: $\left|\ +1 \quad -1\ \right\rangle$ and $\left|\ -1 \quad +1\ \right\rangle$, where the first term in the vector $\left|\ \sigma \quad l\ \right\rangle$, $\sigma = \pm 1$, is the direction of the polarization circularity or the spin, whereas the second term $l = \pm 1$ is the topological charge of the partial vortex. Moreover, the spin and the topological charge of the beam in the crystal are strongly connected with each other. This is a universal property of partial optical vortices in crystals similar to that of guided vortices in optical fibers [26]. As the mode beam propagates along the crystal, the "weight" coefficients of the partial vortices change. However, only at the plane $z = 0$, the beam can contain the single local vortex $\left|\ -1 \quad +1\ \right\rangle$ in the $\tilde{\Psi}_1$ field (or $\left|\ +1 \quad -1\ \right\rangle$ in the $\tilde{\Psi}_2$ field), while there is a pair of these vortices in the beam in other cross-sections of the crystal. This means that, for example, the initial singular beam $\left|\ -1 \quad +1\ \right\rangle$ in free space at the input of the crystal can be transformed into two partial vortices $\left|\ -1 \quad +1\ \right\rangle$ and $\left|\ +1 \quad -1\ \right\rangle$ in the crystal. We can select a single partial vortex after the crystal with a polarized filter consisting of a quarter-wave plate and a polarizer.

Generation of Optical Vortices

Consider now the propagation of a left-hand circularly polarized fundamental Gaussian beam

$$\mathbf{G}_0 = \hat{\mathbf{c}}^-\frac{1}{Z}\exp\left(ik\frac{r^2}{2Z}\right)$$

through the crystal. The field of this beam cannot be presented as a superposition of the TM and TE modes. However, in real optical crystals, $|\Delta\varepsilon\,/\,\varepsilon| \ll 1$ and we can use the perturbation theory for solving Eq. (4). By writing

$$\tilde{\mathbf{E}}_t = \mathbf{E}^{(0)} + \alpha\,\mathbf{E}^{(1)} + \alpha^2\mathbf{E}^{(2)} + ..., \qquad (10)$$

where $\mathbf{E}^{(0)}$ satisfies the equation

$$\left(\nabla_t^2 + 2\,i\,k\,\partial_z\right)\,\mathbf{E}^{(0)} = 0, \qquad (11)$$

where $\alpha = \Delta\varepsilon\,/\,\varepsilon$, we find for the first order of the perturbation theory:

$$\left(\nabla_t^2 + 2\,i\,k\,\partial_z\right)\,\mathbf{E}^{(1)} = -\,\nabla_t\left(\nabla_t\,\mathbf{E}^{(0)}\right)\,. \qquad (12)$$

The solution of (12) can be found by putting

$$\mathbf{E}^{(1)} = \nabla_t\,\Phi\,(x,y,z)\,, \qquad (13)$$

which gives

$$\left(\nabla_t^2 + 2\,i\,k\,\partial_z\right)\,\Phi = -\,\nabla_t\,\mathbf{E}^{(0)}\,. \qquad (14)$$

Having in mind the incidence of a fundamental Gaussian beam on the crystal from the isotropic medium, we consider the left-hand circular polarization $E_x^{(0)} = G_0$, $E_y^{(0)} = i\,G_0$.

Then we come to the equation:

$$\left(\nabla_t^2 + 2\,i\,k\,\partial_z\right)\,\Phi = -\,\left(\partial_x G_0 + i\,\partial_y G_0\right)\,. \qquad (15)$$

Let us make use of the evident identity:

$$\left(\nabla_t^2 + 2\,i\,k\,\partial_z\right)\,(x\,G_0) \equiv \partial_x G_0,$$

$$\left(\nabla_t^2 + 2\,i\,k\,\partial_z\right)\,(y\,G_0) \equiv \partial_y G_0, \qquad (16)$$

whence the potential Φ in Eq. (14) is

$$\Phi = -\frac{1}{2}\,(x + i\,y)\,G_0 \qquad (17)$$

and the first correction $\mathbf{E}^{(1)}$ is

$$\mathbf{E}^{(1)} = \nabla_t\,\Phi\ =$$

$$= -\left\{\hat{\mathbf{c}}^+ ik\frac{(x+i\,y)^2}{4Z} + \hat{\mathbf{c}}^-\left(1 + ik\frac{r^2}{4\,Z}\right)\right\}G_0. \qquad (18)$$

The total field in the crystal found from Eqs.(10) and (18) is

$$\tilde{\mathbf{E}} = \left\{-\,\hat{\mathbf{c}}^+ ik\,\alpha\,\frac{(x+i\,y)^2}{4Z} + \right.$$

$$\left. \hat{\mathbf{c}}^-\left[1 - \alpha\,\left(1 + ik\frac{r^2}{4\,Z}\right)\right]\right\}G_0. \qquad (19)$$

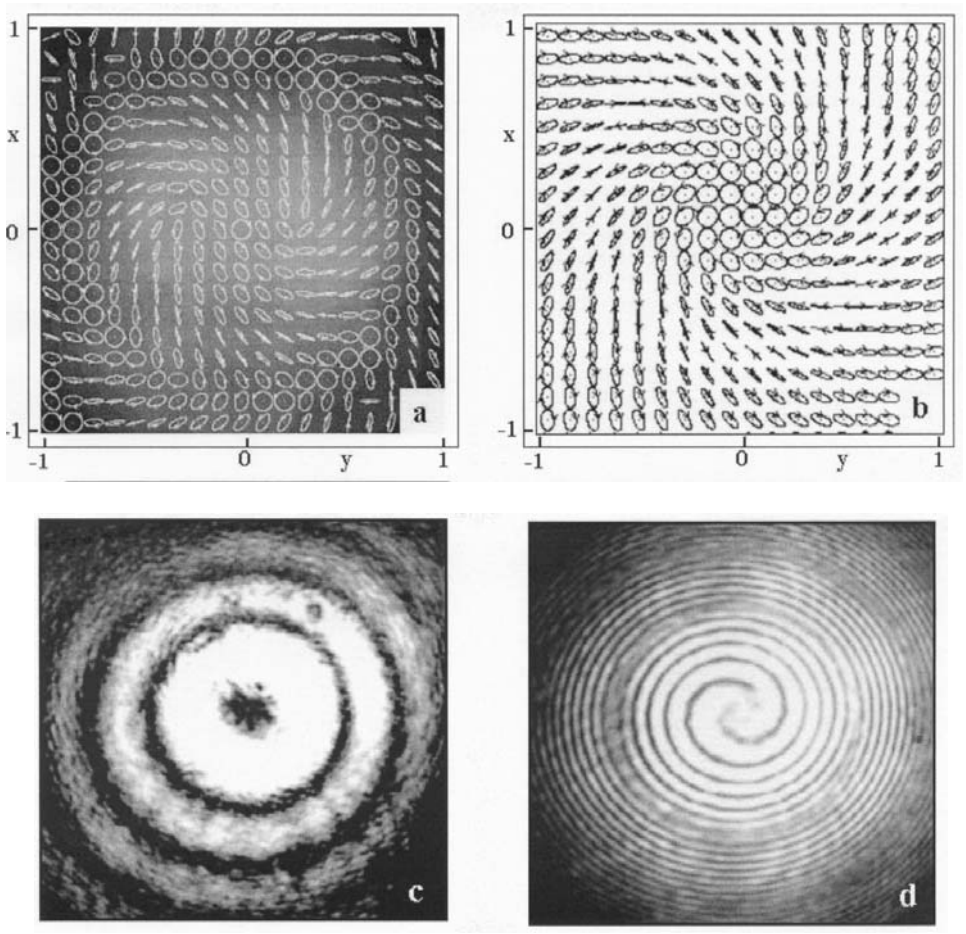

Fig.2. Generation of a singular beam in $LiNbO_3$ crystal: *a* — the experimentally obtained map of the beam polarization state against a background of the beam intensity distribution after the crystal; *b* — the same map calculated on the base of Eq. (19); *c* — the intensity distribution of the singular beam bearing the double charged optical vortex after the polarized filter and *d* — its interference pattern

Similarly, we can find the wave function of a right-hand circularly polarized beam:

$$\tilde{\mathbf{E}} = \left\{ \hat{\mathbf{c}}^{+} \left[1 - \alpha \left(1 + ik\frac{r^2}{4Z} \right) \right] - \right.$$

$$\left. - \hat{\mathbf{c}}^{-} ik\,\alpha\, \frac{(x - i\,y)^2}{4Z} \right\} G_0. \qquad (20)$$

Thus, as a paraxial circularly polarized Gaussian beam transmits through the uniaxial crystal along its optical axis, a part of energy converts into a singular beam with the orthogonal circular polarization bearing an optical vortex with a double topological charge. Namely, the right-hand circularly polarized beam generates the optical vortex with a negative topological charge, whereas the left-hand one generates a positively charged vortex nested in the induced singular beam.

A physical mechanism of this process elucidates the map of polarization states of the beam after $LiNbO_3$ crystal shown by Fig. 2,*a*. This map was experimentally obtained by means of a differential polarimeter. The beam at the crystal input is right-hand circularly polarized. A set of ellipses on the picture forms a typical pattern of a degenerate umbilic point [23] with spiral-like branches. The central point corresponds to the circular polarization of the initial beam. One round of the point is accompanied by twisting of ellipses axes by an angle of 2π. This means that the major

beam contains two coherent local beams with orthogonal circular polarizations, one of the beams having a phase singularity with double topological index at the axis. The recondite singular beam can be selected by suppressing the first beam. A quarter-wave plate and a polarizer can perform it. The quarter-wave plate transforms the initial circular polarization into a linear one, while the polarizer crushes down the first beam, as is demonstrated in Fig 2,*b*. The double interference spiral shown by Fig.2,*d* points out the double topological charge of the vortex.

It should also be added that the degenerate umbilic is a very unstable one. Experimentally, we can split it into two elementary ones by placing a lop-sided quarter-wave plate just after the crystal. This process is illustrated by Fig. 3,*a*. Instead of the degenerate spiral umbilic, we now observe two spatially parted patterns in the form of "lemon" umbilics [23] positioned near the beam axis (Fig.3,*b*,*c*). Far from the axis there is the "star" umbilic (Fig.3,*d*). The polarized filter cuts out the combined singular beam carrying over two optical vortices with the same charges.

We can easily theoretically obtain the result being in good agreement with the experiment by acting the matrix of the polarized-wave plate, whose axis is parallel to the laboratory x-axis, while its phase difference is $\Delta \ll 1$ [24]:

$$\hat{\Delta} = \begin{pmatrix} 1 & i\frac{\Delta}{2} \\ i\frac{\Delta}{2} & 1 \end{pmatrix} \tag{21a}$$

on the field vector of Eq. (18). The pattern depicted in Fig.4,*d* is a result of the computer simulation of this destructive process.

For estimating the field structure near the single umbilic, we make use of Eq. (18) in the form:

$$E^{+} \approx -i\,A\,(x+i\,y)^2, \quad E^{-} \approx 1, \tag{21b}$$

where we consider the crystal length $z = d$ to be much larger than z_0 and $A \approx \alpha\, k/4d$. By operating matrix (21a) on vector (21b), we find

$$E^{+}_{\rm pert} = \left(-iA\,(x+i\,y)^2 + i\frac{\Delta}{2}\right) G_0 \quad , \quad E^{-}_{\rm pert} \approx G_0. \tag{21c}$$

The phase perturbation displaces a position of the field zero $E^{+}_{\rm pert} = 0$ so that

$$A\,(x_0^2 - y_0^2) + \Delta/2 = 0, \quad 2\,x_0 y_0 = 0,$$

whence the coordinates of the field zero are

$$x_0 = 0, \quad y_0 = \pm\sqrt{\frac{\Delta}{2\,A}}. \tag{21d}$$

Let us displace the origin in Eq. (21c) to the point given by Eq. (21d):

$$\tilde{E}^{+}_{\rm pert} \approx -\sqrt{2\,A\,\Delta}\;(x' + i\,y')\,G_0, \quad \tilde{E}^{-}_{\rm pert} \approx G_0. \tag{21e}$$

(Eq. (21e) corresponds to (+) sign in Eq. (21d).)

By using Eq. (21e), one can write Stokes' parameters in the circularly polarized basic [24]:

$$S_2 = 2\,{\rm Re}\left\{{\rm E}^{+}_{\rm pert}\left({\rm E}^{-}_{\rm pert}\right)^{*}\right\} = -2\sqrt{2\,{\rm A}\,\Delta}\,{\rm x}'|{\rm G}_0|^2,$$

$$S_3 = 2\,{\rm Im}\left\{{\rm E}^{+}_{\rm pert}\left({\rm E}^{-}_{\rm pert}\right)^{*}\right\} = -2\sqrt{2\,{\rm A}\,\Delta}\,{\rm y}'|{\rm G}_0|^2,$$

where the star (*) stands for a complex conjugation.

The axis of a polarized ellipse is inclined at the angle

$${\rm tg}\,2\psi = \frac{S_3}{S_2} = \frac{y'}{x'} = {\rm tg}\,\varphi.$$

where φ is an azimuth angle in the polar coordinates.

Thus, the ellipse axis is directed along the line

$$\psi = \frac{\varphi}{2}$$

at each point of the observation plane.

On the other hand, the set of envelopes in the field of directions is defined by the equation:

$$\frac{d\,r}{r\,d\,\varphi} = {\rm tg}\,\frac{\varphi}{2}$$

so that the integral curve is

$$r = \frac{C}{\cos^2\frac{\varphi}{2}}, \tag{21f}$$

where $C = {\rm const}$.

The last equation presents the polarized "lemon" umbilic shown in Fig.4. A similar equation can be found for the point $x_0 = 0$, $y_0 = -\sqrt{\Delta/2A}$. The distance between the two "lemon" umbilics associated with two optical vortices is $h = 2\sqrt{\Delta/2A}$.

The "star" umbilic positioned farther from the center than the "lemon" on the experimental pattern of Fig.3,*d*, can not be found in the network of our approximate theory.

Since the vortex displacement in the perturbed field is proportional to $\sqrt{\Delta}$, we can operate the radial position of the singularity by changing the external perturbation.

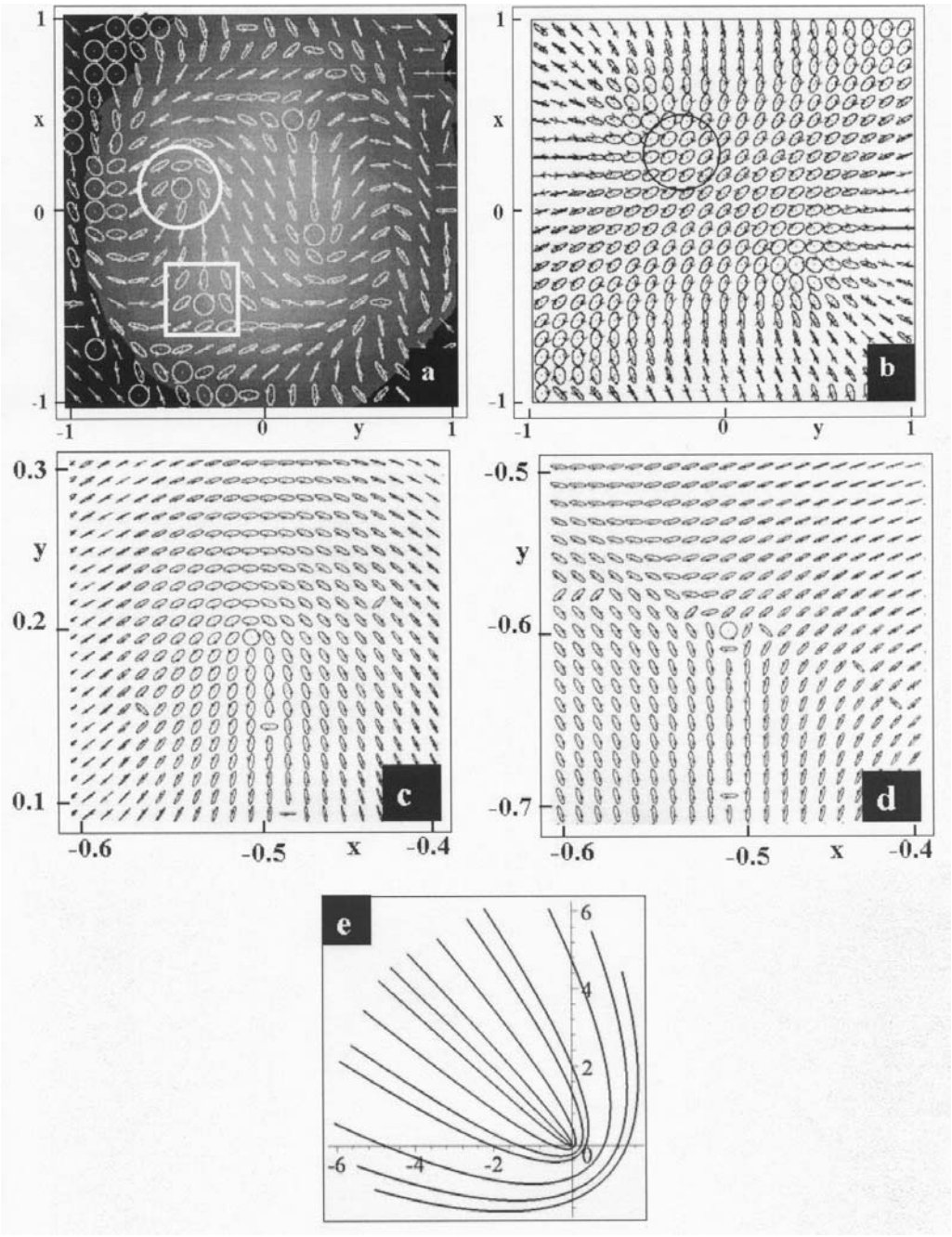

Fig.3. Splitting of the degenerate umbilic: *a* — the experimentally obtained map of the polarization state against the background of a beam perturbed by the lop-sided quarter-wave plate; *b* — the same map calculated on the base of Eq. (21c) in which the circlet cuts down the vicinity of the "lemon" umbilic (*c*) while the small square points out the "star" umbilic (*d*); the theoretically calculated current lines near the "lemon" umbilic

An angular vortex position can be shown to depend linearly on the orientation angle φ of the quarter-wave plate axis or the polarizer axis in the polarized filter [17]. These enable to uniquely perform a vortex displacement over all the beam cross-section.

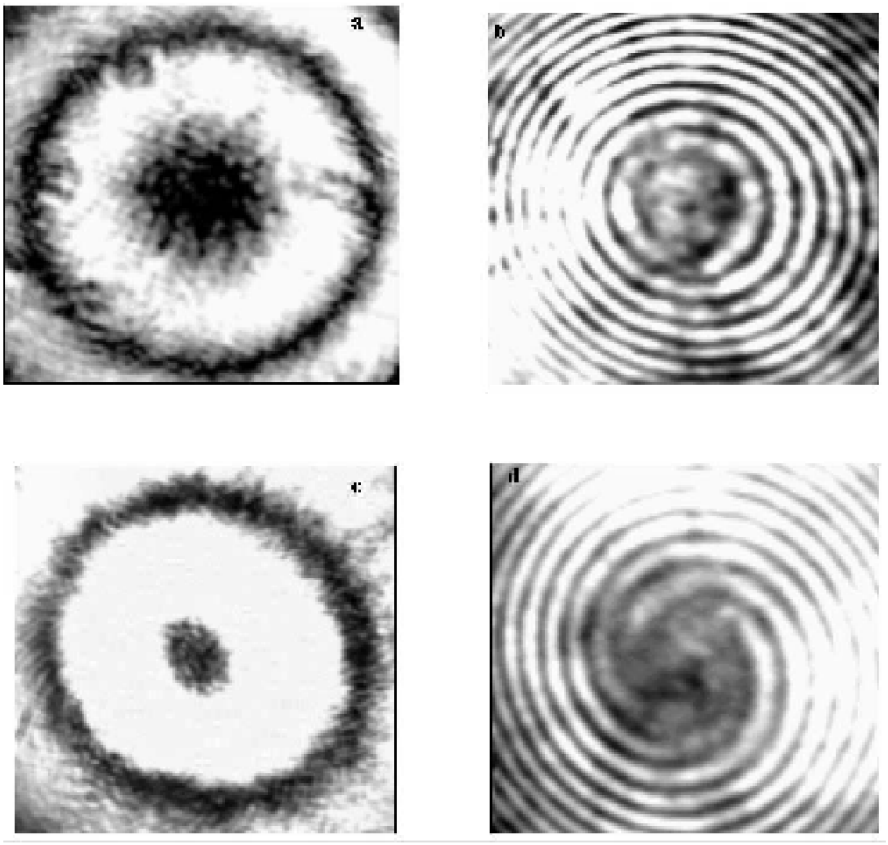

Fig. 4. Conversion of the singular beam: *a* — the intensity distribution of the right-hand circular polarization bearing a positive double topological charge after the polarized filter; *b* — unfolding of the phase singularities manifesting itself in the form of the concentric interference rings; *c* — changing of the handedness of the initial circular polarization causes the transformation of the intensity distribution, and *d* — the interference pattern in which the number of the spiral branches becomes equal to four

When the phase perturbation is vanished, $\Delta = 0$, the equation for the envelopes is written as

$$r = C \exp(-\varphi).$$

This expression describes the set of logarithmic spirals depicted by Fig. 2,*b* that illustrate the spiral degenerate umbilic. Thus, we can regard the degenerate umbilic in the beam emitted from the crystal as a critical point [28] of the vector field after the crystal.

Conversion of Optical Vortices in Crystal

The analysis mentioned above is not restricted with a description of only the singular beam generation, but can be extended to the processes of conversion of a high-order singular beam. Indeed, identities (16) also take place for high-order paraxial Gaussian beams with the wave function

$$G_l = \left(\frac{x + i\kappa y}{Z}\right)^l G_0, \qquad (22)$$

$\kappa = \pm 1$.

However, the final result is very sensitive to picking out of an initial polarization state and the sign of the topological charge.

Let us take again an initial beam in the form of the left-hand circular polarization with a positive topological charge $\kappa = +1$, i.e. $\mid -1, \quad +l \rangle$ state. In this case, the potential Φ has the same form as that in Eq. (17), and

solution (10) is written as

$$\tilde{\mathbf{E}} = \begin{pmatrix} E^+ \\ E^- \end{pmatrix} = \begin{pmatrix} -\alpha\ ik\frac{(x+iy)^{l+2}}{2Z^{l+1}} \\ l+1-\alpha\ ik\frac{r^2}{2Z}\left(\frac{x+iy}{Z}\right)^l \end{pmatrix} G_0 =$$

$$= \begin{pmatrix} -\alpha\ ik\frac{(x+iy)^2}{2Z^1} \\ l+1-\alpha\ ik\frac{r^2}{2Z} \end{pmatrix} G_l. \qquad (23)$$

Thus, the topological charge of the E^+component raises by two units: $l \Rightarrow l+2$.

Much the same result we can obtain is subjected to changing the signs at both the topological charge and the polarization circularity (or the spin) of the initial beam, i.e. $\mid +1, \quad -l \rangle$ state:

$$\tilde{\mathbf{E}} = \begin{pmatrix} l+1-\alpha\ ik\frac{r^2}{2Z}\left(\frac{x-iy}{Z}\right)^l \\ -\alpha\ ik\frac{(x-iy)^{l+2}}{2Z^{l+1}} \end{pmatrix} G_0. \qquad (24)$$

However, now the optical vortex is generated by a left-hand polarized component, while its topological charge is negative.

Conversion of the singular beams with the same signs of the topological charge and the spin in the initial beam ($|+1,+l\rangle$ and $|-1,-l\rangle$) obeys a little different rule. So, the beam field for the initial state $|-1,-l\rangle$ is

$$\tilde{\mathbf{E}} = \begin{pmatrix} -\alpha\ ik\frac{(x-iy)^{l-2}}{2Z^{l+1}} \\ l+1-\alpha\ ik\frac{r^2}{2Z}\left(\frac{x-iy}{Z}\right)^l \end{pmatrix} G_0, \qquad (25)$$

and, for the state $|+1,+l\rangle$, this is

$$\tilde{\mathbf{E}} = \begin{pmatrix} l+1-\alpha\ ik\frac{r^2}{2Z}\left(\frac{x+iy}{Z}\right)^l \\ -\alpha\ ik\frac{(x+iy)^{l-2}}{2Z^{l+1}} \end{pmatrix} G_0. \qquad (26)$$

Thus, the topological charge is reduced by two units in the E^+component of Eq. (25) and in the E^- component of Eq. (26). The conversion rule for these states is $l \Rightarrow l-2$.

The last rule has one interesting consequence: the fields with states $|+1,+2\rangle$ and $|-1,-2\rangle$ are subjected to the unfolding of phase singularities [23]. A typical experimental pattern is demonstrated by Fig. 4,*a,b* for the initial beam in the state $|+1,+2\rangle$. Although there is a strongly pronounced intensity minimum of the E^-component in Fig.4,*a*, the distinctive "fork" in the interference pattern in Fig. 4,*b* is lacking. This is a graphic evidence for the annihilating of two opposite charged optical vortices in the singular beam. Moreover, a simple rotation of birefringence axes of the quarter-wave plate placed in front of the crystal transforms the initial beam state $|+1,+2\rangle$ into the state $|-1,+2\rangle$. But now the topological charge raising by two units, becomes equal to $l=+4$. It is this effect that is illustrated by Fig. 4,*c,d*. The number of the spiral branches indicates the value of the topological charge, while the spiral winding gives the sign of the vortex charge.

The considered above mode beam transformations underlie the base of action of a new-type mode converter. Indeed, well-known mode converters on the base of astigmatic lenses [25] transform only a vortex topological charge not touching upon a polarization state of the beam. Fiber-optical converters [26, 27] can transform both the topological charge and the polarization state of the guided modes. However, they cannot transform high-order modes, because the conversion process in a multimode fiber is not strongly a determinate one due to a mutual mode conversion caused by random external perturbations. At the same time, the crystal mode converter can easily perform a polarization and a topological charge transformation of both low-order and high-order mode beams.

Conclusions

We have worked out the theory of a paraxial singular beam in the uniaxial crystal and have showed the following.

Propagation of the paraxial Gaussian beam through the crystal along its optical axis is accorded with its transformation into a complicatedly polarized singular beam. However, the beam will preserve its initial polarization provided that its field structure corresponds to that of TM and TM modes.

At the same time, an initial circularly polarized fundamental Gaussian beam can be transformed into a singular beam with double topological charge in one of its components. The sign of the topological charge depends on a polarized circularity of the initial beam. So, a left-hand circularly polarized beam generates the positively charged optical vortex in the right-hand component, while the vortex nested in the left-hand component of the beam after the crystal corresponds to the right-hand circular polarization of the initial beam.

High-order singular beams in the crystal perform a vortex conversion in accordance with the following rule: the states of the initial beam $|+1,\ -l\rangle$ and $|-1,\ +l\rangle$ enlarge the topological charge of the vortex by two units

in the E^- and E^+ components, respectively, while the states $|+1,\ +l\rangle$ and $|-1,\ -l\rangle$ stimulate the diminution of the charge by two units.

This technique of a vortex generation and conversion can find a wide application in microparticle manipulation systems not only as simple vortex generator units but also as those for operating both radial and angular vortex positions.

I am indebted to M. Soskin for bringing the key problems of singular optics to my attention and encouraging my work. I also wish to express my sincere thanks to A. P. Kiselev, V. G. Shvedov and C.N. Aleksiev for their helpful discussions, T. A. Fadeyeva and Yu. A. Egorov for the kindly given experimental results.

1. *Nye J.F., Berry M.V.* // Proc. Roy. Soc. Lond. A. 1974.— **336**.— P.165—190.
2. *Soskin M.S., Vasnetsov M.V.*// Progress in Optics/ Ed. by E. Volf.— 2001.— **42**.— P. 219—276.
3. *Bovin A., Dow J., Wolf E.* // J. Opt. Soc. Amer.— 1967.— **57**, N 10.— P. 1171—1175.
4. *Carter W.H.* // Opt. Communs.— 1973.— **7**, N 3.— P. 211—218.
5. *Born M., Wolf E.* Principles of Optics.— London: Pergamon Press, 1965.— P.P. 405, 406, 532.
6. *Sommerfeld A.* Vorlesungen uber Theoretische Physik. Optik.— Wiesbaden, 1950. — P.22.
7. *Basistiy I.V., Bazhenov V.Yu., Soskin M.S., Vasnetsov M.V.*// Opt. Communs.— 1993.— **103**.— P.422—428.
8. *Basistiy I.V., Soskin M.S., Vasnetsov M.V.*//Ibid.— 1995.— **119**.— P.604—612.
9. *Berry M.* // Proc. SPIE.— 2000.— **4403**.— P. 5—16.
10. *Belyi V.N., King T.A., Kazak N.S. et al.* //Ibid.— P 230—241.
11. *Khilo N.A., Ryzhevich A.A., Petrova E.S.* // Quantum Electronics.— 2001.— **31**,N 1.— P. 85—89.
12. *T.A. King, W. Hogervorst, N.S. Kazak, N.A. et al.* // Opt. Communs.— 2001.— **187**, N 4—6, P.— 407 — 414.
13. *Frins E.M., Ferrari J.A., Dubra A., Perciante D.*// Opt. Lett.— 2000.— **25**, N 5.— P. 284—288.
14. *Stalder M., Schdt M.* //Ibid.— 1996.— **21**, N 23.— P. 1948—1950.
15. *Vlokh R., Volyar A., Mys O., Krupych O.*// Ukr. J. Phys. Opt.— 2003.— **4**, N2.— P.90—93.
16. *Volyar A.V., Fadeyeva T.A.*// Opt. Spektr.— 2003.— **94**, N 2.— P. 235—244.
17. *Volyar A.V., Fadeyeva T.A.* // Ibid.— 2003.— **95**, N 2.— P 285—293.
18. *Volyar A.V., Fadeyeva T.A.*//Ibid.— 2004.— **96**, N 1.— P.108—118.
19. *Ganic D., Gan X., Gu M. et al.* // Opt. Lett.— 2002— **27**, N 15.— P. 1351—1353.
20. *Vinikurov T.N., Rozanov N.I.* // Quantum Electronics.— 1977.— **4**, N 6.— P. 1276—1281.
21. *Volyar A.V., Fadeyeva T.A.* // Opt.Spektr. — 1998.— **85**, N 2.— P. 295—303.
22. *Volyar A.V., Zhilaitis V.Z., Shvedov V.G.* //Ibid.— 1999.— **86**, N 4.— P. 664—670.
23. *Nye J.F.* Natural Focusing and Fine Structure of Light.— Bristol, Philadelphia: Institute of Physics Publishing, 1999.
24. *Azzam R.M.A., Bashara N.M.* Ellipsometry and Polarized Light.— Amsterdam – New-York – Oxford: North-Holland Publishing Company, 1977.— P. 87—104.
25. *Allen L., Padgett M.J., Babiker M.* // Progress in Optics/Ed. by E. Wolf.— 1999.— V. XXXIX.— P.291—372.
26. *Alekseev K.N., Volyar A.V., Fadeyeva T.A.* // Opt. Spectr.— 2002.— **92**, N 4.— P. 5880—597.
27. *Alexeyev C.N., Soskin M.S., Volyar A.V.* // Semiconductor Physics, Quantum Electronics and Optoelectronics.— 2000.— **3**, N 3.— P.501—513.
28. *Freund I., Soskin M.S., Mokhun A.A.I.* // Opt. Communs.— 2002.— **208**.— P. 223—253.

СИНГУЛЯРНІ ПУЧКИ В ОДНОВІСНИХ КРИСТАЛАХ

А.В. Воляр

Р е з ю м е

Розглянуто спосіб генерації сингулярних пучків, що переносять оптичні вихори, в оптичній системі з одновісним кристалом та поляризаційним фільтром. Аналіз розв'язку параксіального хвильового рівняння вказує на те, що лівоциркулярно поляризований гауссів пучок змінюється на неоднорідно поляризований пучок, в якому правоциркулярна компонента поляризації містить оптичний вихор із подвійним позитивним топологічним зарядом. В той час як правоциркулярно поляризований пучок генерує вихор з негативним топологічним зарядом в лівоциркулярно поляризованій компоненті. Крім того, дана система здатна трансформувати заряд вхідного сингулярного пучка: вихор, що переноситься сингулярним пучком з лівою циркуляцією, з позитивним топологічним зарядом збільшує свій заряд на дві одиниці, а в разі однакових знаків заряду вихору та поляризації пучка відбувається зменшення топологічного заряду вихору на дві одиниці. До результатів комп'ютерного моделювання підібрано експериментальні ілюстрації.

To be continued in the next issue